Arabian Journal of Chemistry (2019) **12**, 1322–1337

King Saud University

Arabian Journal of Chemistry

www.ksu.edu.sa
www.sciencedirect.com

SPECIAL ISSUE: ENVIRONMENTAL CHEMISTRY

Adsorption of Basic Magenta II onto H_2SO_4 activated immature *Gossypium hirsutum* seeds: Kinetics, isotherms, mass transfer, thermodynamics and process design

N. Sivarajasekar *, R. Baskar *

Department of Chemical Engineering, Kongu Engineering College, Perundurai, Erode 638052, Tamil Nadu, India

Received 6 June 2013; accepted 29 October 2014
Available online 18 November 2014

KEYWORDS

Gossypium hirsutum seeds;
Isotherms;
Kinetics;
Mass transfer;
Thermodynamics;
Process design

Abstract The adsorption of Basic Magenta II onto H_2SO_4 activated immature *Gossypium hirsutum* seeds was analysed using Ho, modified Freundlich, Sobkowsk–Czerwi, Blanchard, Elovich, Avrami, and modified Ritchie kinetic models by nonlinear regression-sum of normalized errors analysis. The goodness of fit was evaluated with coefficient of determination and root mean square error. The good agreement of experimental data to Avrami second-order model indicated that the mechanism of adsorption followed multiple kinetic orders. The Avrami second-order mechanism was applied to predict the rate constant of sorption and the equilibrium capacity and subsequently the obtained equilibrium adsorption capacities were utilized to find the equilibrium concentrations. Langmuir, Freundlich, Temkin, Sips and Hill isotherms were investigated to understand the nature of adsorption with the help of nonlinear regression analysis. Both Sips and Hill isotherms were best fit to the adsorption equilibrium data showing the homogeneous adsorption on the heterogeneous surface of carbon and the positive co-operative manifestations of the Basic Magenta II molecules. The mass transfer study depicted the details such as mass transfer coefficient, intra-particle diffusion rate, pore diffusion coefficient, and film diffusion coefficient. The adsorption process was found to be controlled by film diffusion. The thermodynamic parameters like, Gibbs free energy change,

* Corresponding authors. Tel.: +91 4294 226600; fax: +91 4294 220087 (N. Sivarajasekar). Tel.: +91 4294 226602; fax: +91 4294 220087 (R. Baskar).
E-mail addresses: sivarajasekar@gmail.com (N. Sivarajasekar), naturebaskar@yahoo.co.in (R. Baskar).
Peer review under responsibility of King Saud University.

Production and hosting by Elsevier

http://dx.doi.org/10.1016/j.arabjc.2014.10.040

enthalpy change, entropy change and isosteric heat of adsorption confirmed the endothermic, feasible and spontaneous nature of adsorption. A single stage batch adsorber was designed using Sips isotherm constants to estimate the amount of carbon required for desired purification.

1. Introduction

Industries such as textile, plastic, tannery, packed food, pulp and paper, paint and electroplating are extensively using more than 10,000 synthetic dyes in their processes (Fu and Viraragvahan, 2002; Radha et al., 2005; Bayramoglu and Yakup Arica, 2007). Since many of the organic dyestuffs are harmful to plant and animal biota, removal of dyestuffs from wastewater has received considerable attention over the past decades. Textile industries are responsible for the discharge of large quantities of dyes into natural water bodies due to the inefficiencies in dyeing techniques (Forgacs et al., 2004). Cationic dyes are extensively used in the textile industry because of their favourable characteristics of bright colour, high solubility in water, simple application technique, and low-energy consumption (Heiss et al., 1992). Among them, Basic Magenta II (BM2) is widely employed in acrylic, wool, nylon and silk dyeing. It may decompose into carcinogenic aromatic amines under anaerobic conditions, so discharge of this dye bearing effluent into water bodies can cause harmful effects such as allergic dermatitis, skin irritation, mutations and cancer (Nawar and Doma, 1989; Roderiguez-Reininoso and Molino Sabio, 1992; Pollard et al., 1992; Srinivasan and Viraraghavan, 2010). Keeping the toxicity of the dye in view there is an urgent need to develop effective methods for its removal from the waste water. Different physicochemical methods like coagulation, ozonation, chemical oxidation, solvent extraction, ion exchange, photo-catalytic degradation, and adsorption have been tried by many researchers for the treatment of dye bearing water. Amid all the methods mentioned, adsorption is an effective and eco-friendly process for colour removal from wastewaters due to its simple design, easy operation and its efficacy to remove a wide range of compounds (Nawar and Doma, 1989; Roderiguez-Reininoso and Molino Sabio, 1992; Pollard et al., 1992). Activated carbon has been extensively utilized as adsorbent in the recent past due to the presence of various oxygenated functional surface groups and its pore structure. Recognizing the high cost of activated carbon, many investigators have attempted for replacing it by cheap, commercially available and renewable bio-based materials (Pollard et al., 1992; Rafatullah et al., 2010; Amran et al., 2011). Some among them include: apricot stones (Philip, 1996), Spirogyra (Sivarajasekar et al., 2008), white oak (Jagtoyen and Derbyshire, 1998), deoiled soya (Gupta et al., 2008), Acacia (Sivarajasekar et al., 2009), date pits (Girgis and Abdel-Nasser, 2002), palm shell (Jia-Guo et al., 2005), cellulose (Zhou et al., 2012), sunflower stalks (Shi et al., 1999), sewage sludge (Martin et al., 2003), olive mill waste (Moreno-Castillaa et al., 2001), Zizania latifolia (Huang et al., 2012), coconut shell (Hu and Srinivasan, 1999), peanut hull (Girgis et al., 2002), lignin (Hayashi et al., 2000), coir pith (Namasivayam and Sangeetha, 2004), corn cob (Tsai et al., 2001), rice husk (Daifullah et al., 2004), walnut shell (Jin-Wha et al., 2001), coffee bean husk (Baquero et al., 2003) and etc.

Adsorption process design demands the insight into the equilibrium adsorption capacity, the mass transfer rate, the rate controlling step and the thermodynamics of the adsorption process. Therefore, it is important to have information relating to the rate of dye removal, the liquid phase diffusion coefficients, Gibbs free energy, enthalpy and entropy of the system (Ofomaja, 2011; Sivarajasekar and Baskar, 2014).

Even though many agricultural and waste materials were used as adsorbents for the removal of colour, adsorbent derived from immature *Gossypium hirsutum* seeds were never reported yet to the best of our knowledge. Therefore an attempt was made to prepare adsorbent from immature *G. hirsutum* seeds via chemical activation and to examine its ability of up-taking BM2 from aqueous solution. The experimental data resulting from batch adsorption experiments were analysed by using two-parameter (Ho, modified Freundlich, and Sobkowsk–Czerwi) and three-parameter (Blanchard, Elovich, Avrami, and modified Ritchie) kinetic models. The equilibrium data pertained to the well-fitting kinetic models were adopted for examine the suitability of five different isotherms (Langmuir, Freundlich, Temkin, Sips and Hill). Sum of normalized errors and statistical comparison values were applied to find a best fitting isotherm. The feasibility of the adsorption process under various temperatures was studied and a single stage batch adsorber was designed.

2. Materials and methods

2.1. Chemicals

Basic Magenta II (also called Basic red 9, molecular weight = 337.86, chemical formula $C_{20}H_{20}ClN_3$ and λ_{max} = 550 nm) was obtained from Hi Media Laboratories Ltd, Mumbai. All other chemicals used were obtained from Merck India Ltd, Mumbai. The structure of BM2 is shown in Fig. 1.

2.2. Preparation of dye solution

The stock solution of BM2 was prepared by dissolving 1 g of dye in 1 l of doubly distilled water. All working solutions were

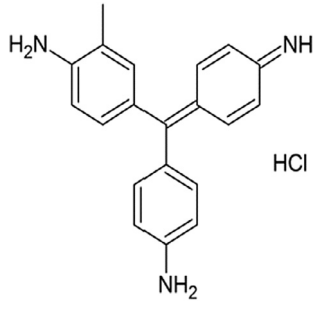

Figure 1 Structure of BM2.

prepared by diluting the stock solution with doubly distilled water to the desirable concentration. The initial pH of working solution was adjusted to the required value by adding 0.1 N HCl or 0.1 N NaOH solutions before mixing the adsorbent with the dye solution. The concentration of dye in the sample was analysed using a double beam UV–Vis spectrophotometer (ELICO-SL244, India) at a maximum wavelength of 550 nm.

2.3. Activated carbon preparation

Immature *G. hirsutum* seeds were collected from *G. hirsutum* seed producers near Attur, Tamil Nadu, India. The collected seeds were washed thoroughly with distilled water to remove dirt and dried at 40 °C in a temperature controlled oven for 3 days. The dried biomass was soaked with 98% concentrated sulphuric acid in the weight ratio of 1:4 (1 g *G. hirsutum* seed: 4 g H_2SO_4). In order to achieve effective activation the acid soaked biomass was stirred periodically and kept for 12 h. The resultant slurry was carefully washed with doubly distilled water. Further, the traces of acid were removed by washing the material twice with 0.1 N sodium bicarbonate solution. The resultant material, immature *G. hirsutum* seed activated carbon (IGHSAC) was dried, finely ground sieved with 170 mesh and stored in an air tight container to subsequently use it in the batch adsorption experiments.

2.4. The characterization of IGHSAC

The iodine number and methylene blue number of IGHSAC was calculated based on the ASTM 4607-86 standards at 298 K (Moreno-Castillaa et al., 2001). To measure iodine number, 0.1 g of carbon was washed initially by 5% HCl solution and agitated with 100 ml of 0.1 N iodine solution until equilibrium reached. The residual iodine concentration in the aqueous phase was determined by titrating with 0.1 N sodium thiosulphate solution taking starch as an indicator. Methylene blue number was determined by agitating 0.1 g of carbon with 10 ml of 150 mg l^{-1} methylene blue solution. The concentration of methylene blue was analysed using a double beam UV–Vis spectrophotometer (ELICO-SL244, India) at 665 nm. The specific surface area of IGHSAC was determined from the adsorption–desorption isotherm of nitrogen 77 K using a surface analyser (Micromeritics ASAP 2020). 1 g of carbon was added to 100 ml of deionized water and agitated for 2 h and the pH of the slurry was noted subsequently as the pH of carbon. The bulk density of the carbon was measured using a pycnometer.

2.5. Batch adsorption

Batch adsorption studies were conducted for the selected concentration range (50–250 mg l^{-1}), at the pH of 12, IGHSAC dosage of 5 g and contact time of 3 h. The thermodynamic studies were carried at four different temperatures (20–40 °C). Each experiment were carried out by agitating 5 g of adsorbent with 200 ml of dye solution taken in Erlenmeyer flasks and agitating them using a thermo-regulated shaker (GeNei SLM-IN-OS-16, India) operating at 100 rpm. The samples were withdrawn from the flasks at predetermined time intervals for kinetic studies and at equilibrium time for isotherm studies. Obtained samples were centrifuged for 2 min (Remi R-24 Centrifuge, India) to remove the suspended solids. The clear supernatants were analysed for the residual dye concentration using double beam UV–Vis spectrophotometer (ELICO-SL244, India). The dye adsorption capacity q_t (mg g^{-1}) was determined as

$$q_t = (C_0 - C_t) \times \frac{V}{M} \tag{1}$$

where C_0 (mg l^{-1}) and C_t (mg l^{-1}) are initial and final concentration of BM2, V (l) is volume of dye solution, and M (g) is amount of IGHSAC.

2.6. Nonlinear error analysis

Frequently, by linear regression magnitude of the coefficient of determination (R^2) is the index to measure the quality of the fit to the batch adsorption data. However, transformation of non-linear equations into linear ones utterly upset their error structure and may defy the error variance of normality assumptions of standard least squares (Myers, 1990; Ratkowski, 1990). Additionally linear regression is not always a good choice to apply for equations with more than two parameters and therefore the non-linear regression analysis is preferable to determine isotherm and kinetic parameters (Ho, 2006; Kumar and Sivanesan, 2007; Ncibi, 2008). Generally, the optimization procedure required an error function to be able to evaluate the fit of the equation to the experimental data and the parameters derived can be affected by the choice of the error function (Hanna and Sandall, 1995; Ho, 2004; Sivarajasekar and Baskar, 2013). Various error functions employed are:

$$\text{Sum of the square error (ERRSQ)} : \sum_{i=1}^{p} (q_{t,meas} - q_{t,calc})_i^2 \tag{2}$$

$$\text{Derivative of hybrid fractional error function (HYBRID)} : \sum_{i=1}^{p} \left[\frac{(q_{t,meas} - q_{t,calc})^2}{q_{t,meas}} \right]_i \tag{3}$$

$$\text{Derivative of Marquardt's percentage standardright deviation (MPSD)} : \sum_{i=1}^{p} \left(\frac{q_{t,meas} - q_{t,calc}}{q_{t,meas}} \right)_i^2 \tag{4}$$

$$\text{Average relative error (ARE)} : \sum_{i=1}^{p} \left| \frac{q_{t,meas} - q_{t,calc}}{q_{t,meas}} \right|_i \tag{5}$$

$$\text{The sum of absolute errors (EABS)} : \sum_{i=1}^{p} \left| q_{t,meas} - q_{t,calc} \right|_i \tag{6}$$

where $q_{t,meas}$ is adsorption capacity from experiment (mg g^{-1}), $q_{t,calc}$ is adsorption capacity calculated from models (mg g^{-1}), $\overline{q_{t,calc}}$ is mean adsorption capacity calculated from models (mg g^{-1}), n is number of data points, p is number of variables in the models. The statistical comparison values such as coefficient of determination (R^2) and root mean square error (RMSE) can also be utilized to gauge the goodness of the fit.

Coefficient of determination (R^2)

$$: \frac{\left(q_{t,meas} - \overline{q_{t,calc}}\right)_i^2}{\sum_{i=1}^{p}\left(q_{t,meas} - \overline{q_{t,calc}}\right)^2 + \left(q_{t,meas} - q_{t,calc}\right)^2} \tag{7}$$

Root mean square error(RMSE)

$$: \sqrt{\frac{1}{p-2}\sum_{i=1}^{p}\left(q_{t,meas} - q_{t,calc}\right)^2} \tag{8}$$

These error functions and statistical comparison values can be evaluated using the tools like *solver* add-in with Microsoft's spread sheet, Excel (Microsoft™, 1995) through any of the iteration methods. The application of these five different error methods will produce different parameter sets; therefore, it is hard to recognize an overall optimum parameter set. In order to facilitate a meaningful comparison between the isotherms parameter sets, the procedure of 'sum of the normalized errors' (SNE) is usually adopted (Ho et al., 2002; Foo and Hameed, 2010). This approach allows a direct comparison of the scaled errors and thus identifies the parameter set that would provide the closest fit to the measured data. The parameter set derived based on the smallest SNE will be an optimal one providing that there is no bias in the data sampling and type of error functions selected.

3. Result and discussion

3.1. Characterization of IGHSAC

Iodine number is an index of pores with diameter ranging from 10 to 28 Å usually falls in the microporous range (< 20 Å) which is 510 mg g^{-1} in our case. The development of micro pores on the IGHSAC was depicted by methylene blue number since the molecular diameters of its molecules were 15 Å (Kasaoka et al., 1981; Rajgopal et al., 2006) and was measured to be 42 mg g^{-1}. These results demonstrated that good amount of meso and micro-pores were developed on the surface of IGHSAC. The larger BET surface area (496.5 m^2 g^{-1}) also indicated the suitability of the carbon for dye adsorption. The pH and bulk density of IGHSAC were found to be 6.5 and 0.56 g ml^{-1} respectively.

3.2. Kinetics

The kinetics of solute sorption is required for selecting optimum operating conditions for the full-scale batch process. The kinetic parameter, which is supportive for the prediction of adsorption rate and equilibrium time, gives important information for designing and modelling the processes (Sivarajasekar and Baskar, 2014). Therefore various kinetic equations including two-parameter kinetic models: Ho, modified Freundlich, and Sobkowsk–Czerwi, and three-parameter kinetic models: Blanchard, Elovich, Avrami and modified Ritchie were employed for testing the experimental batch data.

The pseudo-second order model proposed by Ho and McKay Ho (1995) describes that adsorption process is controlled by chemisorption which involve valence forces through sharing or exchange of electron between the solute and the adsorbent. The Ho pseudo-second order model can be represented in the following form:

$$q_t = \frac{q_e^2 k_{Ho} t}{1 + k_{Ho} q_e t} \tag{9}$$

where k_{Ho} (g mol^{-1} min^{-1}) is the rate constant of pseudo-second-order model which can be useful to calculate the initial sorption rate h (mg g^{-1} min^{-1}), as follows:

$$h = k_{Ho} q_e^2 \tag{10}$$

The modified Freundlich equation was authored by Kuo and Lotse (Yeddou et al., 2010):

$$q_t = k_{mF} C_i t^{1/m_{mF}} \tag{11}$$

where k_{mF} (l g^{-1} min^{-1}) is the apparent adsorption rate constant, and m is the Kuo–Lotse constant. The values of k_{mF} and m_{mF} were used empirically to evaluate the effect of solute surface loading and ionic strength on the adsorption process.

Blanchard et al. (1984) postulated a second order kinetic model assuming that the solute adsorption on the adsorbent follows ion exchange mechanism. Blanchard model is given as

$$q_t = \frac{k_{Bla} q_e t + \alpha_{Bla} q_e - 1}{k_{Bla} t + \alpha_{Bla}} \tag{12}$$

where k_{Bla} (min^{-1}) is Blanchard kinetic rate constant and α_{Bla} is Blanchard model constant. This model reduces to Ho model when α_{Bla} is equal to $1/q_e$.

Elovich equation is also used successfully to describe second-order kinetic assuming that the actual solid surfaces are energetically heterogeneous (Sparks, 1989). It can be expressed in the following form:

$$q_t = \beta_E \ln(r_E \beta_E) + \beta_E t \tag{13}$$

where r_E (mg g^{-1} min^{-1}) is the initial adsorption rate, and the β_E (g mg^{-1}) is related to the extent of surface coverage and activation energy for chemisorption.

The Avrami kinetic equation determines some kinetic parameters as possible changes of the adsorption rates in terms of the initial concentration and the adsorption time in addition to the determination of fractional kinetic orders (Ho and McKay, 2003). Avrami kinetic equation can be written as follows:

$$q_t = q_e[1 - \exp(-k_{Av} t)^{n_{Av}}] \tag{14}$$

where k_{Av} (min^{-1}) is Avrami rate constant and n_{Av} is Avrami model exponent of time which is related to the adsorption mechanism changes.

Ritchie Cheung et al. (2000) proposed a method for the second-order kinetic adsorption of gases on solids. He assumed that the rate of adsorption of solute onto adsorbent depends solely on the fraction of surface sites (θ), which are occupied by adsorbed gas. It is in the following form:

$$\theta = \frac{q_t}{q_e} = \left\{1 - \left[\frac{1}{\beta_R + k_R t}\right]\right\} \tag{15}$$

where k_R (min^{-1}) is the Ritchie rate constant and β_R is Ritchie model constant that represents initial particle loading.

A second order kinetic model proposed by Sobkowsk and Czerwi (1974) similar to Ritchie model based on the maximum adsorption capacity of adsorbents. Modified form of this model is expressed as:

$$q_t = \frac{q_e k_{SC} t}{k_{SC} + 1} \tag{16}$$

Table 1 Error functions and sum of normalized errors for two-parameter kinetic models.

Model	mg l^{-1}	Error	ERRSQ	HYBRID	MPSD	ARE	EABS	SNE
Ho	50	ERRSQ	22.3468	4.7342	1.0093	308.5801	6.6829	3.5667
		HYBRID	22.3634	4.7311	1.0078	322.0540	6.7026	3.6085
		MPSD	22.3931	4.7325	1.0075	331.2050	6.7183	3.6386
		ARE	30.9312	7.0483	1.6816	1.2106	10.4308	4.0037
		EABS	22.3611	4.7419	1.0115	299.6484	6.6662	3.5410
	100	ERRSQ	74.9121	8.7297	1.0246	1480.1194	12.5231	2.7544
		HYBRID	75.1613	8.7050	1.0165	1605.5157	12.5883	2.8275
		MPSD	75.8342	8.7249	1.0143	1729.8864	12.8883	2.9175
		ARE	134.1080	19.0450	2.9461	1.4763	23.4501	4.0009
		EABS	75.6107	8.7793	1.0285	1409.0183	12.1714	2.7074
	150	ERRSQ	140.4267	12.0263	1.0489	3534.2949	19.3342	2.2254
		HYBRID	141.4099	11.9574	1.0333	3917.6051	19.7431	2.3230
		MPSD	143.8280	12.0054	1.0294	4281.3157	20.2839	2.4287
		ARE	371.8521	39.7576	4.6940	1.6532	38.9594	4.0004
		EABS	141.1182	12.0878	1.0552	3360.3023	19.0288	2.1816
	200	ERRSQ	201.3342	14.5810	1.0909	6242.1883	25.8244	1.9433
		HYBRID	204.2498	14.4172	1.0612	7112.2548	26.9882	2.0715
		MPSD	211.0993	14.5234	1.0541	7930.3395	28.1096	2.2056
		ARE	705.3114	63.9697	6.5253	1.8133	54.2971	4.0002
		EABS	201.9511	14.7051	1.1048	6110.7429	25.6104	1.9277
	250	ERRSQ	250.2930	16.6285	1.1708	8638.5911	31.6771	1.7171
		HYBRID	258.3165	16.2356	1.1015	10308.1780	33.6771	1.8801
		MPSD	280.4568	16.5536	1.0826	12164.3708	36.1812	2.0919
		ARE	1097.8707	94.3783	9.3008	1.8550	66.4301	4.0002
		EABS	259.3445	17.9343	1.3079	7069.6256	29.5030	1.5922
Modified Freundlich	50	ERRSQ	7.5164	1.2471	0.2343	1.0839	7.3385	4.2252
		HYBRID	8.0940	1.1439	0.1804	1.1447	7.8032	4.0816
		MPSD	9.5161	1.2183	0.1662	1.2182	8.4023	4.3229
		ARE	11.7261	1.5187	0.2199	1.0664	8.2778	4.7990
		EABS	11.7261	1.5187	0.2199	1.0664	8.2778	4.7990
	100	ERRSQ	30.1599	3.0995	0.3872	1.1777	14.5730	3.8198
		HYBRID	33.9540	2.7181	0.2655	1.3119	16.3713	3.7207
		MPSD	44.1554	3.0253	0.2314	1.4286	18.2035	4.0967
		ARE	51.5664	4.2151	0.4427	1.0989	16.0071	4.6486
		EABS	51.5664	4.2151	0.4427	1.0989	16.0071	4.6486
	150	ERRSQ	77.9923	5.6361	0.5222	1.3547	23.4823	3.8234
		HYBRID	89.2511	4.8068	0.3293	1.4211	25.0174	3.5039
		MPSD	117.8740	5.4120	0.2792	1.5668	28.2596	3.8481
		ARE	180.1224	7.7414	0.3955	1.3260	29.4367	4.6036
		EABS	180.1224	7.7414	0.3955	1.3260	29.4367	4.6036
	200	ERRSQ	150.9835	8.9024	0.6963	1.5750	33.5465	3.8179
		HYBRID	176.1100	7.3643	0.4016	1.6200	35.0094	3.3962
		MPSD	235.8934	8.3648	0.3314	1.7318	38.6744	3.6865
		ARE	373.5733	12.2453	0.4776	1.5545	43.1610	4.5836
		EABS	373.5733	12.2453	0.4776	1.5545	43.1610	4.5836
	250	ERRSQ	250.1842	13.8550	1.0556	1.7469	42.8212	3.9884
		HYBRID	303.2859	10.9561	0.5463	1.8300	45.1907	3.5925
		MPSD	427.2599	12.7589	0.4297	2.0641	52.0711	4.1398
		ARE	329.9922	16.4088	1.1863	1.7114	47.4313	4.5124
		EABS	329.9922	16.4088	1.1863	1.7114	47.4313	4.5124
Sobkowsk–Czerwi	50	ERRSQ	1.7346	0.2735	0.0471	0.4635	3.1787	4.5144
		HYBRID	1.7686	0.2672	0.0444	0.4916	3.3176	4.5566
		MPSD	1.8213	0.2696	0.0439	0.5085	3.3951	4.6392
		ARE	1.7862	0.2979	0.0538	0.4316	3.0287	4.6375
		EABS	1.9275	0.3071	0.0532	0.4404	3.0045	4.7395
	100	ERRSQ	4.4363	0.3796	0.0370	0.4337	5.3676	4.7356
		HYBRID	4.7084	0.3525	0.0293	0.4319	5.6819	4.5562
		MPSD	5.2904	0.3679	0.0276	0.4329	5.9839	4.7134
		ARE	4.4465	0.3759	0.0361	0.4319	5.3480	4.6969
		EABS	4.4478	0.3765	0.0362	0.4322	5.3456	4.7018

(*continued on next page*)

Table 1 (*continued*)

Model	mg l^{-1}	Error	ERRSQ	HYBRID	MPSD	ARE	EABS	SNE
	150	ERRSQ	15.5782	0.8948	0.0604	0.5884	10.1711	3.1047
		HYBRID	16.6689	0.8172	0.0447	0.5520	10.2837	2.8146
		MPSD	18.6960	0.8811	0.0443	0.5420	10.1183	2.8630
		ARE	48.8244	1.7840	0.0699	0.7088	17.2444	5.0000
		EABS	18.2662	0.9307	0.0533	0.5762	9.9353	3.0484
	200	ERRSQ	38.7241	1.8840	0.1089	0.7758	16.3030	4.6795
		HYBRID	42.1379	1.6867	0.0763	0.7379	16.7572	4.3208
		MPSD	48.8244	1.7840	0.0699	0.7088	17.2444	4.4320
		ARE	51.8429	1.9084	0.0738	0.7138	16.7120	4.5668
		EABS	42.9718	1.8741	0.0950	0.7701	15.9875	4.6032
	250	ERRSQ	74.8624	3.4933	0.2067	0.9776	22.8631	1.4751
		HYBRID	84.7954	2.9916	0.1278	0.9371	23.6881	1.3974
		MPSD	106.9245	3.2886	0.1101	0.9072	24.9595	1.4623
		ARE	124.8696	3.8435	0.1229	0.8932	23.4636	1.5135
		EABS	80.7063	3.3892	0.1805	0.9570	21.7202	1.4283

where k_{SC} (min^{-1}) is Sobkowsk–Czerwi second order kinetic rate constant.

Batch experiments were carried out for differential concentrations (50–250 mg l^{-1}) with pH 12, temperature 40 °C, and contact time 3 h. The resulting experimental data was analysed on the basis of the nonlinear curve fitting SNE procedure by minimizing one error function and calculating all other error values. The determined SNE values for the two-parameter and three parameter kinetic models are displayed in Tables 1 and 2 respectively. Error functions which contribute minimum SNE value were selected to calculate the optimum parameter set for that kinetic model. From Table 1, it was inferred that the HYBRID error function produced the best fit giving the lowest SNE value for the 14 cases out of the 35 cases studied followed by the MPSD error function for 9 cases and EABS error function for 7 cases. Additionally, the ERRSQ error function selected to measure optimum parameter set for 4 cases and ARE error function provided optimum parameter set for only one case. The values of optimum parameter sets calculated based on minimum SNE procedure and their coefficient of determination (R^2) and root mean square error (RMSE) values are presented in Tables 3 and 4 in order to assess the fitness of the kinetic models.

Among the two-parameter kinetic models, the Sobkowsk–Czerwi model provided a better fit to the experimental data with high R^2 (0.9996–0.95596) and low RMSE (0.9313–6.51135) values than Ho and modified Freundlich models at studied concentration range. This conveyed an idea that the adsorption may be followed first order kinetics at low concentrations and second order kinetics at high concentrations (Ho, 2006). As for as three-parameter kinetic models concerned, the Avrami kinetic model followed by modified Ritchie kinetic model had a good agreement with the experimental batch data which was known from their high R^2 and low RMSE values (Table 4). The applicability of Avrami kinetic model (R^2: 0.9997–0.9789, RMSE: 0.7388–4.5028) indicated that the mechanism of adsorption certainly followed multiple kinetic orders which may change during the contact of the dye with IGHSAC (Lopes et al., 2003). The modified Ritchie kinetic model also reasonably explained the experimental data (R^2: 0.9996–0.9537, RMSE: 0.9299–6.6785) which conveyed the idea that dye molecules were adsorbed onto two different surface sites. The higher initial dye uptake at small time duration (< 30 min) was most likely due to certain active surface sites on IGHSAC; and quickly adsorption becoming dependent on the diffusion controlling process which had good agreement with the conclusion arrived by Sobkowsk–Czerwi kinetic model. The poor R^2 and high RMSE values of Elovich and modified Freundlich kinetic models were shown that these models failed to explain the experimental data. According to the R^2 and RMSE values the best-fitted kinetic models were found in the order: Avrami > Sobkowsk–Czerwi > modified Ritchie > Blanchard > Elovich > modified Freundlich > Ho. Therefore the q_e values predicted by the Avrami kinetic model were considered for the isotherm calculations.

3.3. Isotherms

To optimize the design of an adsorption system for the removal of solutes by adsorbents, it is important to establish the most appropriate correlation for the equilibrium curves. Adsorption isotherm provides valuable information such as equilibrium sorption capacity and certain constants whose values express the surface properties and affinity of the adsorbent (Sivarajasekar and Baskar, 2013). In many cases, the equilibrium sorption capacity is unknown, chemisorption tends to become immeasurably slow, and the amount sorbed is still significantly smaller than the equilibrium amount (Ungarish and Aharoni, 1981). This problem can be easily rectified if the equilibrium adsorption capacity (q_e) and equilibrium concentration (C_e) values owing to the well-fitting kinetic models are adopted for isotherm fitting (Ho, 2004; Ho and Wang, 2004). Therefore the amount of dye adsorbed at equilibrium predicted from the Avrami kinetic model was considered for isotherm studies. The equilibrium solute phase concentration in liquid can be calculated from the Eq. (1) as follows:

$$C_e = C_0 - \frac{q_e M}{V} \tag{17}$$

The predicted equilibrium data from Avrami kinetics were fitted to the five isotherm models to understand the nature of adsorption process. The most widely used two-parameter isotherm models (Langmuir, Freundlich and Temkin) and three-parameter isotherm models (Sips and Hill) isotherms were used to describe the equilibrium nature of adsorption.

Table 2 Error functions and sum of normalized errors for three-parameter kinetic models.

Model	mg l^{-1}	Error	ERRSQ	HYBRID	MPSD	ARE	EABS	SNE
Blanchard	50	ERRSQ	1.7294	0.2727	0.0471	1.4653	3.2469	3.4819
		HYBRID	1.8246	0.2659	0.0453	1.4971	3.6140	3.5630
		MPSD	2.1831	0.2787	0.0433	1.5059	3.9503	3.7267
		ARE	4.7498	0.3675	0.0710	1.4062	4.3927	4.9338
		EABS	1.9274	0.3070	0.0531	1.4402	3.0041	3.6298
	100	ERRSQ	4.3284	0.3584	0.0343	1.4172	5.5263	3.8209
		HYBRID	12.1444	0.2748	0.0258	1.3729	7.6204	4.1163
		MPSD	6.5332	0.2911	0.0243	1.3820	6.6580	3.6455
		ARE	15.8644	0.3336	0.0324	1.3087	7.4013	4.6035
		EABS	4.4846	0.3863	0.0378	1.4352	5.3141	3.9800
	150	ERRSQ	15.0981	0.8269	0.0538	1.5559	10.3938	4.1137
		HYBRID	28.6658	0.6496	0.0401	1.5014	12.8107	4.2774
		MPSD	18.5863	0.6953	0.0370	1.5023	11.4678	3.8399
		ARE	30.7659	0.7545	0.0488	1.4354	12.0114	4.5072
		EABS	17.7611	0.9384	0.0568	1.5849	9.9385	4.3531
	200	ERRSQ	37.2914	1.7157	0.0949	1.7225	16.5662	4.0454
		HYBRID	55.7791	1.3858	0.0716	1.6860	19.3906	4.0088
		MPSD	43.4845	1.5097	0.0647	1.6949	18.0008	3.7938
		ARE	82.2779	1.8045	0.1085	1.5561	18.9616	4.7939
		EABS	42.0898	1.9181	0.1029	1.7778	15.9470	4.2820
	250	ERRSQ	71.0119	3.0311	0.1673	1.9069	23.4122	3.1197
		HYBRID	120.0957	2.1843	0.1046	1.8240	27.7817	3.0601
		MPSD	89.2053	2.4365	0.0922	1.8267	25.7124	2.8884
		ARE	260.6857	3.3831	0.2009	1.6309	29.6347	4.0874
		EABS	84.9210	4.9311	0.3450	1.9915	21.3419	4.0459
Elovich	50	ERRSQ	5.2231	0.7757	0.1290	0.8910	6.1417	4.3843
		HYBRID	5.5004	0.7211	0.1019	0.8781	6.2510	4.1527
		MPSD	5.9943	0.7450	0.0968	0.8688	6.3769	4.2077
		ARE	8.1326	0.9546	0.1168	0.7898	6.6073	4.7913
		EABS	8.1326	0.9546	0.1168	0.7898	6.6073	4.7913
	100	ERRSQ	17.8296	1.5163	0.1574	0.9363	11.7461	3.3747
		HYBRID	19.4156	1.3359	0.1034	0.9222	12.1978	3.0851
		MPSD	22.2886	1.4124	0.0939	0.8878	12.4445	3.0874
		ARE	59.2559	3.3537	0.1938	0.7505	14.5141	4.8016
		EABS	59.2559	3.3537	0.1938	0.7505	14.5141	4.8016
	150	ERRSQ	44.4300	2.5024	0.1775	1.0206	18.0873	4.5687
		HYBRID	48.0622	2.1867	0.1105	0.9155	17.5873	3.9993
		MPSD	53.2981	2.2790	0.1015	0.8641	17.7674	4.0188
		ARE	67.7654	2.7407	0.1149	0.7678	17.8257	4.3854
		EABS	67.7654	2.7407	0.1149	0.7678	17.8257	4.3854
	200	ERRSQ	83.8736	3.7261	0.2084	1.1587	25.3543	4.6983
		HYBRID	90.0337	3.2574	0.1300	1.0321	24.6666	4.1174
		MPSD	96.2185	3.3368	0.1228	0.9709	24.4774	4.0968
		ARE	115.1053	3.8430	0.1405	0.9187	25.2402	4.4625
		EABS	115.1053	3.8430	0.1405	0.9187	25.2402	4.4625
	250	ERRSQ	137.4871	5.5355	0.2957	1.2868	32.0210	4.8294
		HYBRID	149.6143	4.6755	0.1665	1.1230	31.0469	4.1526
		MPSD	159.4578	4.7819	0.1571	1.0922	31.1064	4.1773
		ARE	165.7731	4.9110	0.1647	1.0365	31.3582	4.2291
		EABS	165.7731	4.9110	0.1647	1.0365	31.3582	4.2291
Avrami	50	ERRSQ	1.0799	0.2385	0.0558	0.4810	2.3240	4.7632
		HYBRID	1.0937	0.2364	0.0543	0.4799	2.3738	4.7568
		MPSD	1.1807	0.2421	0.0534	0.4935	2.5922	4.9497
		ARE	1.0917	0.2385	0.0555	0.4701	2.2404	4.7141
		EABS	1.0968	0.2405	0.0562	0.4704	2.2210	4.7323
	100	ERRSQ	1.2452	0.1440	0.0191	0.2991	2.8811	4.6309
		HYBRID	1.2676	0.1421	0.0183	0.2879	2.7922	4.5205
		MPSD	1.4230	0.1481	0.0177	0.2818	2.8610	4.6255
		ARE	1.6350	0.1657	0.0187	0.2704	2.8119	4.8603
		EABS	1.3120	0.1434	0.0179	0.2787	2.7228	4.4814
	150	ERRSQ	4.2171	0.2596	0.0195	0.3426	5.3723	4.9405
		HYBRID	4.2287	0.2589	0.0195	0.3419	5.3300	4.9322
		MPSD	4.2558	0.2606	0.0194	0.3406	5.3272	4.9357
		ARE	4.3776	0.2634	0.0196	0.3383	5.2260	4.9602
		EABS	4.3702	0.2632	0.0196	0.3384	5.2313	4.9575

(*continued on next page*)

Table 2 (*continued*)

Model	mg l^{-1}	Error	ERRSQ	HYBRID	MPSD	ARE	EABS	SNE
	200	ERRSQ	15.4295	0.7430	0.0406	0.4748	10.0595	4.4188
		HYBRID	15.8842	0.7187	0.0377	0.5000	10.4413	4.4477
		MPSD	16.3989	0.7241	0.0374	0.5119	10.6113	4.5175
		ARE	16.4741	0.8729	0.0509	0.4382	9.4878	4.7008
		EABS	16.7287	0.8876	0.0518	0.4364	9.4451	4.7426
	250	ERRSQ	37.7549	1.6084	0.0814	0.6407	16.1939	3.8527
		HYBRID	40.5510	1.4787	0.0627	0.6046	16.2903	3.6848
		MPSD	46.7315	1.5579	0.0583	0.6360	16.9567	3.8980
		ARE	41.5862	1.4862	0.0615	0.5974	16.3152	3.6922
		EABS	49.1227	2.5013	0.1484	0.6832	16.1157	4.9504
Modified Ritchie	50	ERRSQ	1.7294	0.2727	0.0471	0.4653	3.2469	3.3499
		HYBRID	1.8246	0.2659	0.0453	0.4971	3.6140	3.4696
		MPSD	2.1831	0.2787	0.0433	0.5059	3.9503	3.6361
		ARE	5.2202	0.3742	0.0725	0.4046	4.5083	4.7997
		EABS	1.7842	0.2975	0.0537	0.4318	3.0281	3.4028
	100	ERRSQ	4.3284	0.3584	0.0343	0.4172	5.5263	3.3381
		HYBRID	12.1444	0.2748	0.0258	0.3729	7.6204	3.6686
		MPSD	6.5332	0.2911	0.0243	0.3820	6.6580	3.2119
		ARE	15.8268	0.3334	0.0323	0.3086	7.3942	3.9796
		EABS	5.3605	0.4864	0.0504	0.4522	5.1642	4.0164
	150	ERRSQ	15.0981	0.8269	0.0538	0.5559	10.3938	4.0634
		HYBRID	28.6658	0.6496	0.0401	0.5014	12.8107	4.1276
		MPSD	18.5863	0.6953	0.0370	0.5023	11.4678	3.7184
		ARE	33.5572	0.7659	0.0506	0.4312	12.2375	4.4195
		EABS	17.5334	0.9289	0.0564	0.5810	9.9767	4.3013
	200	ERRSQ	37.2914	1.7157	0.0949	0.7225	16.5662	4.0079
		HYBRID	37.2914	1.7157	0.0949	0.7225	16.5662	4.0079
		MPSD	43.4845	1.5097	0.0647	0.6949	18.0008	3.7396
		ARE	82.4417	1.8057	0.1086	0.5560	18.9683	4.6417
		EABS	41.8344	1.9422	0.1065	0.7810	15.9325	4.3284
	250	ERRSQ	71.0119	3.0310	0.1673	0.9069	23.4123	3.7203
		HYBRID	71.0119	3.0310	0.1673	0.9069	23.4123	3.7203
		MPSD	89.2052	2.4366	0.0922	0.8267	25.7124	3.5946
		ARE	71.0119	3.0310	0.1673	0.9069	23.4123	3.7203
		EABS	84.9422	4.9337	0.3452	0.9916	21.3418	4.7822

Table 3 Kinetic parameters and statistical comparison values for two-parameter models at various initial concentrations.

Model	Parameters	50 mg l^{-1}	100 mg l^{-1}	150 mg l^{-1}	200 mg l^{-1}	250 mg l^{-1}
Ho	k_{Ho} (g mol^{-1} min^{-1})	0.0147	0.0057	0.0031	0.0019	0.0019
	q_e (mg g^{-1})	9.8533	19.1758	28.9351	39.1651	45.3490
	h (mg g^{-1} min^{-1})	1.4243	2.1137	2.6297	2.9427	3.8318
	R^2	0.9944	0.9669	0.9054	0.8613	0.8653
	RMSE	3.3437	6.1486	8.3999	10.0487	11.3874
Modified Freundlich	m_{mf}	4.5722	3.8264	3.3890	3.0372	2.7955
	k_{mf} (l g^{-1} min^{-1})	0.0669	0.0535	0.0446	0.0367	0.0309
	R^2	0.9980	0.9851	0.9401	0.8791	0.8425
	RMSE	2.0117	4.1203	6.6802	9.3838	12.3143
Sobkowsk–Czerwi	k_{SC} (min^{-1})	0.1204	0.0883	0.0717	0.0589	0.0516
	q_e (mg g^{-1})	10.0259	20.2402	30.5166	40.5816	49.9508
	R^2	0.9996	0.9979	0.9888	0.9711	0.9559
	RMSE	0.9313	1.5343	2.8869	4.5901	6.5114

According to the Langmuir isotherm, the monolayer adsorption is taking place on a structurally homogeneous adsorbent where all the adsorption sites are identical and energetically equivalent (Langmuir, 1918). Langmuir Isotherm is:

$$q_e = \frac{q_{mL} b_L C_e}{1 + b_L C_e} \tag{18}$$

where $q_{mL} = K_L/b_L$ (mg g^{-1}) is the maximum monolayer adsorption capacity predicted by Langmuir isotherm, K_L

Table 4 Kinetic parameters and statistical comparison values for three-parameter models at various initial concentrations.

Model	Parameter	50 mg l^{-1}	100 mg l^{-1}	150 mg l^{-1}	200 mg l^{-1}	250 mg l^{-1}
Blanchard	α_{Bla}	0.0121	0.0048	0.0026	0.0015	0.0012
	k_{Bla} (min^{-1})	0.0991	0.0462	0.0310	0.0235	0.0188
	q_e (mg g^{-1})	10.0198	20.0332	30.2298	40.3710	49.3585
	R^2	0.9996	0.9971	0.9875	0.9701	0.9537
	RMSE	0.9299	1.8074	3.0485	4.6629	6.6785
Elovich	r_E (mg g^{-1} min^{-1})	4.0432	4.5626	4.9665	4.7349	5.2836
	β_E (g mg^{-1})	0.5842	0.2604	0.1633	0.1142	0.0931
	R^2	0.9986	0.9915	0.9678	0.9339	0.9223
	RMSE	1.6584	3.1157	4.9022	6.9361	8.6491
Avrami	n_{Av}	0.2885	0.2680	0.2478	0.2340	0.2215
	k_{Av} (min^{-1})	0.2885	0.2680	0.2478	0.2340	0.2215
	q_e (mg g^{-1})	9.0534	17.8317	26.4046	34.6730	42.1618
	R^2	0.9997	0.9994	0.9971	0.9894	0.9789
	RMSE	0.7388	0.8100	1.4782	2.7775	4.5028
Modified Ritchie	b_R	0.9931	0.9245	0.9367	0.9505	0.9260
	k_R (min^{-1})	0.1212	0.0966	0.0775	0.0620	0.0570
	q_e (mg g^{-1})	10.0198	20.0332	30.2298	40.3710	49.3586
	R^2	0.9996	0.9971	0.9875	0.9701	0.9537
	RMSE	0.9299	1.8074	3.0485	4.6629	6.6785

($l\,g^{-1}$) and b_L ($l\,mg^{-1}$) are the Langmuir model constants. Weber and Chakravorti (1974) proposed a separation factor (R_L) to understand the favorability of isotherm that should be less than one for favourable adsorption, defined as

$$R_L = \frac{1}{1 + C_0 b_L} \tag{19}$$

The empirical Freundlich isotherm model describes the non-ideal and reversible nature of adsorption. The multilayer adsorption with non-uniform distribution of adsorption heat and affinities over the heterogeneous surface explained by its relationship (Adamson and Gast, 1997):

$$q_e = K_F C_e^{1/n_F} \tag{20}$$

where K_F ($l\,g^{-1}$) is the Freundlich isotherm constant, and n_F is Freundlich exponent. The value $1/n_F < 1$ indicates chemisorption process, whereas $1/n_F > 1$implies cooperative adsorption (Haghseresht and Lu, 1998).

The isotherm postulated by Temkin and Pyzhev (1940) relates the effects of heat of adsorption that decreases linearly with the coverage of the solute and the adsorbent interactions on the surface at moderate values of solute concentrations. It is represented by:

$$q_e = \frac{RT}{b_T}\{\ln(a_T C_e)\} \tag{21}$$

where b_T ($J\,mol^{-1}$) is the Temkin isotherm constant related to heat of sorption, a_T ($l\,g^{-1}$) is the Temkin isotherm constant, R is the gas constant (8.314 $J\,mol^{-1}\,K^{-1}$) and T (K) is the absolute temperature.

Sips (1948) proposed a combined form of Langmuir and Freundlich isotherms deduced for predicting the heterogeneous adsorption systems. At low solute concentrations it effectively reduces to Freundlich isotherm and at high solute concentrations, it predicts characteristics of monolayer sorption capacity of the Langmuir isotherm. Sips isotherm is given by

$$q_e = \frac{K_S q_{mS} C_e^{1/n_S}}{1 + K_S C_e^{1/n_S}} \tag{22}$$

where K_S ($l\,g^{-1}$) is the Sips isotherm constant, q_{mS} (mg g^{-1}) is the maximum monolayer adsorption capacity by Sips isotherm, and n_S is the Sips model exponent.

Hill (1910) postulated an isotherm to describe the binding of different solutes onto a homogeneous adsorbent. The model assumes that adsorption is a cooperative occurrence, owing to the ligand binding ability at one site on the macromolecule, tends to influence different binding sites on the same macromolecule. The Hill equation is:

$$q_e = \frac{q_{mH} C_e^{n_H}}{K_H + C_e^{n_H}} \tag{23}$$

where q_{mH} (mg g^{-1}) is the maximum monolayer adsorption capacity given by Hill isotherm, K_H is the Hill isotherm Constant and n_H is Hill cooperativity coefficient. If $n_H > 1$, positive cooperativity in binding, $n_H = 1$, non-cooperative or hyperbolic binding, and $n_H < 1$, negative cooperativity in binding.

Nonlinear SNE procedure was adopted to evaluate the optimum parameters for the five types of isotherms. The error functions, SNE values and optimum parameters are presented in Tables 5 and 6. The HYBRID error function produced optimum parameter set for all the selected isotherms due to their small SNE values. By analysing the R^2 and RMSE values of the isotherm models, the best fitting was observed using Sips (R^2: 0.9945, RMSE: 0.5492) and Hill (R^2: 0.9945, RMSE: 0.5494) isotherms. The Langmuir isotherm (R^2: 0.9918, RMSE: 0.6731) reasonably fitted the data followed by Freundlich isotherm (R^2: 0.9183, RMSE: 2.1254) but Temkin isotherm failed to define the equilibrium data well. The adequacy of Sips and Hill isotherms confirmed that the homogeneous adsorption on the heterogeneous surface of IMSAC and the co-operative manifestations of the adsorptive BM2 molecules. The maximum adsorption capacity predicted by

Table 5 Error functions and sum of normalized errors for isotherms.

S. No.	Isotherm		ERRSQ	HYBRID	MPSD	ARE	EABS	SNE
1.	Langmuir	ERRSQ	0.8493	0.0385	0.0019	0.0834	1.8543	4.6053
		HYBRID	0.9061	0.0355	0.0015	0.0730	1.8684	4.2504
		MPSD	0.9931	0.0364	0.0015	0.0729	1.9353	4.3530
		ARE	1.1345	0.0428	0.0017	0.0702	1.7832	4.6403
		EABS	0.9855	0.0411	0.0019	0.0803	1.7951	4.6840
2.	Freundlich	ERRSQ	7.5182	0.4197	0.0333	0.2928	5.8773	4.3728
		HYBRID	9.0342	0.3307	0.0166	0.2408	5.7892	3.6112
		MPSD	12.8966	0.3846	0.0131	0.2346	6.4597	4.0026
		ARE	10.0446	0.4769	0.0317	0.2850	5.5803	4.5686
		EABS	10.1167	0.4744	0.0311	0.2831	5.5669	4.5410
3.	Temkin	ERRSQ	13.2476	0.8414	0.0663	0.4699	7.1560	4.3267
		HYBRID	15.8049	0.6896	0.0376	0.3614	7.8047	3.6700
		MPSD	24.0371	0.7986	0.0320	0.3308	8.7519	4.0959
		ARE	18.4299	0.8783	0.0448	0.2697	7.0094	3.8178
		EABS	13.3339	0.8427	0.0650	0.4581	7.0039	4.2693
4.	Sips	ERRSQ	0.5415	0.0329	0.0023	0.0828	1.3775	3.9045
		HYBRID	0.6032	0.0290	0.0016	0.0740	1.5357	3.6103
		MPSD	0.7937	0.0318	0.0014	0.0725	1.7705	3.9426
		ARE	0.8725	0.0490	0.0028	0.0591	1.0789	4.3235
		EABS	0.5641	0.0356	0.0025	0.0809	1.2727	3.9801
5.	Hill	ERRSQ	0.5415	0.0328	0.0023	0.0827	1.3784	3.9305
		HYBRID	0.6038	0.0290	0.0016	0.0740	1.5362	3.6365
		MPSD	0.7936	0.0318	0.0014	0.0725	1.7702	3.9705
		ARE	0.8640	0.0484	0.0027	0.0521	1.0060	4.1986
		EABS	0.5643	0.0354	0.0025	0.0806	1.2732	4.0040

Table 6 Parameters and statistical comparison values for isotherms.

S. No.	Isotherm	Parameters		R^2	RMSE
1.	Langmuir	q_{mL} (mg g^{-1})	86.24	0.9918	0.6731
		b_L (l g^{-1})	0.02		
		R_L	0.22		
2.	Freundlich	K_F (mg g^{-1}) (l $g^{-1})^n_F$	3.30	0.9183	2.1254
		n_F	1.42		
3.	Temkin	a_T (l g^{-1})	0.37	0.8571	2.8111
		b_T (J mol^{-1})	174.80		
4.	Sips	q_{mS} (mg g^{-1})	77.76	0.9945	0.5492
		b_S	0.03		
		n_S	0.95		
5.	Hill	q_{mH} (mg g^{-1})	77.78	0.9945	0.5494
		n_H	1.05		
		K_H	39.71		

the Sips (77.76 mg g^{-1}) and Hill (77.78 mg g^{-1}) isotherms were lower than Langmuir (86.24 mg g^{-1}) isotherm. The value of Sips exponent ($0.95 \approx 1$) conveyed the idea that the sorption data was more of a Langmuir form rather than that of Freundlich isotherm. In turn, Freundlich isotherm almost fitted to the equilibrium data supporting the assumptions of heterogeneous mode of adsorption to certain extend. The Hill exponent n_H was greater than unity (1.05) depicted that the binding interaction between BM2 molecule and IGHSAC was in the form of positive cooperativity. The separation factor (R_L) value determined from the Langmuir isotherm indicated that dye adsorption onto IMSAC was in favourable region ($R_L < 1$). Fig. 2 collectively represents all the isotherm models.

3.4. Sorption mechanisms

The knowledge of the rate-limiting step is an important one to be considered in the adsorption process. It is governed by the adsorption mechanism which depends on the physical and chemical characteristics of the adsorbent as well as on the mass transfer process (Metcalf and Eddy, 2003). For a solid–liquid sorption process, the solute transfer is usually characterized

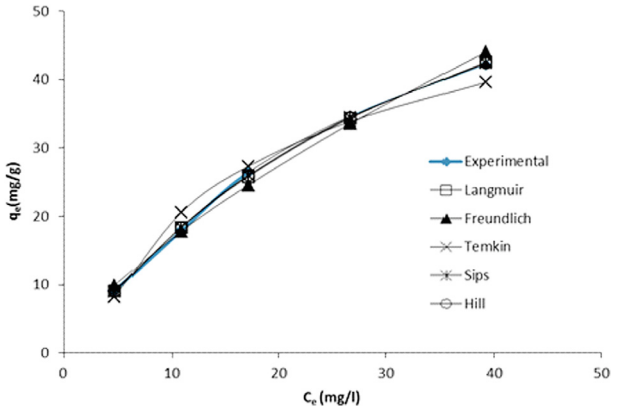

Figure 2 Comparison of isotherms.

by external mass transfer or intraparticle diffusion, or both. The three steps involved in the mechanism of adsorption as follows:

(1) Transport of the solute from bulk solution through boundary layer to the adsorbent exterior surface (film diffusion);
(2) Transport of the solute within the pores of the adsorbent (particle diffusion);
(3) Adsorption of the solute on the exterior surface of the adsorbent (equilibrium reaction).

Usually, the last step is very rapid; the resistance is therefore assumed to be negligible. The slowest step determines the rate-controlling parameter in the adsorption process. Yet, the rate-controlling parameter may be distributed between intraparticle and film diffusion mechanisms. Irrespective of the case external diffusion will be involved in the sorption process. In general, external diffusion or external mass transfer is characterized by the initial solute uptake (McKay et al., 1981) which can be calculated from the slope of Furusawa and Smith plot assuming a linear relation between C_t/C_i and time for the first initial rapid phase (Vadivelan and Kumar, 2005). That is,

$$\left[\frac{d(C_t/C_0)}{dt}\right]_{t\to 0} = -k_m S \tag{24}$$

where k_m (cm s^{-1}) is external mass transfer coefficient and S (cm^2/cm^3) is surface area of the adsorbent per unit volume of particle which is defined as:

$$S = \frac{6M}{V d_p \rho (1-\varepsilon_p)} \tag{25}$$

where d_p is particle diameter (cm), ρ is bulk density (g cm^{-3}) and ε_p is porosity. The external mass transfer rate values were determined at different initial concentrations of BM2 using Fig. 3(a) and presented in Table 7. The slopes of the curves were calculated based on the assumption that the relationship is linear for the first initial rapid period of time (< 30 min). As seen, the external mass transfer rates decreased with increasing initial concentration of dye may be due to the nature of molecular associations or interionic groups present in the dye; which may reduce the activity coefficient of the dye and effective diffusivity (McKay et al., 1981).

The common technique used for identifying the mechanism involved in the adsorption process is described by Weber and Morris (1963) via fitting a plot for the following equation:

$$q_t = K_{id} t^{0.5} \tag{26}$$

where K_{id} is intraparticle diffusion rate constant (mg g^{-1} min$^{-0.5}$). Therefore to realize the exact diffusion mechanism, q_t values were plotted against $t^{0.5}$ and presented in Fig. 3(b). As seen, the two stages in the intraparticle diffusion plot suggested that the sorption process proceeded by surface sorption and intraparticle diffusion. The initial curved portion of the plot indicated that at first, BM2 molecules diffused through the surrounding boundary layer to the external surface of the IGHSAC particles. The later linear portion is attributed to intraparticle or pore diffusion of BM2 molecules to the adsorptive active sites located on the IGHSAC particles. Therefore intraparticle diffusion rate constant K_{id} was calculated from the slope of the second linear portion of the plot and is listed in Table 7. The intraparticle diffusion rate constants seemed to increase with increasing initial BM2 concentrations, perhaps as a result of a raise in the concentration gradient leading to a rapid upturn in the driving force for the mass transfer. On the other hand, the intercept of the plot reflected the idea that intraparticle diffusion was not only rate controlling one but boundary layer diffusion also controlled the adsorption of BM2 to some extent. The larger the value of intercept, the greater is the contribution of the surface sorption in the rate-controlling step. The boundary layer diffusion rate constants (k_f) were obtained as the intercept of the second portion of the plot and presented in Table 7.

To understand the diffusion mechanism quantitatively and to estimate the rate determining step (pore diffusion or film diffusion), it is prerequisite to calculate their coefficients. By assuming the adsorbent particle to be a sphere of radius 'r' and the diffusion follows Fick's law, the adsorption kinetic data was further analysed using the relationship between fractional attainment of equilibrium and time according to Reichenberg and Helfferich (Reichenberg, 1953; Vadivelan and Kumar, 2005):

$$\frac{q_t}{q_e} = 6\left(\frac{D_t}{r^2}\right)^{0.5}\left[\pi^{-0.5} + 2\sum_{n=1}^{\infty} ierfc\left(\frac{\pi r}{D^{0.5}}\right) - 3\left(\frac{D}{r^2}\right)\right] \tag{27}$$

At smaller times (t tends to 0) D is substituted by D_f and Eq. (18) reduces to:

$$\frac{q_t}{q_e} = 6\left(\frac{D_t}{r^2}\right)^{0.5} t^{0.5} \tag{28}$$

where D_f (cm^2 s^{-1}) is film diffusion coefficient. The fractional uptake (q_t/q_e) values were plotted against square root of time ($t^{0.5}$) (Fig. 3(c)) and the calculated film diffusion coefficients D_f are listed in Table 7. At larger times (t tends to ∞) Eq. (27) can be written as:

$$\frac{q_t}{q_e} = 1 - \left[\frac{6}{\pi^2}\sum_{n=1}^{\infty}\frac{1}{n^2}\exp\left(-\frac{n^2\pi^2 D_p t}{r^2}\right)\right] \tag{29}$$

where D_p (cm^2 s^{-1}) is pore diffusion coefficient. If the Biot number $B = (D_p\pi^2/r^2)$, Eq. (29) can be simplified to:

$$Bt = -0.4977 - \ln\left(1 - \frac{q_t}{q_e}\right) \tag{30}$$

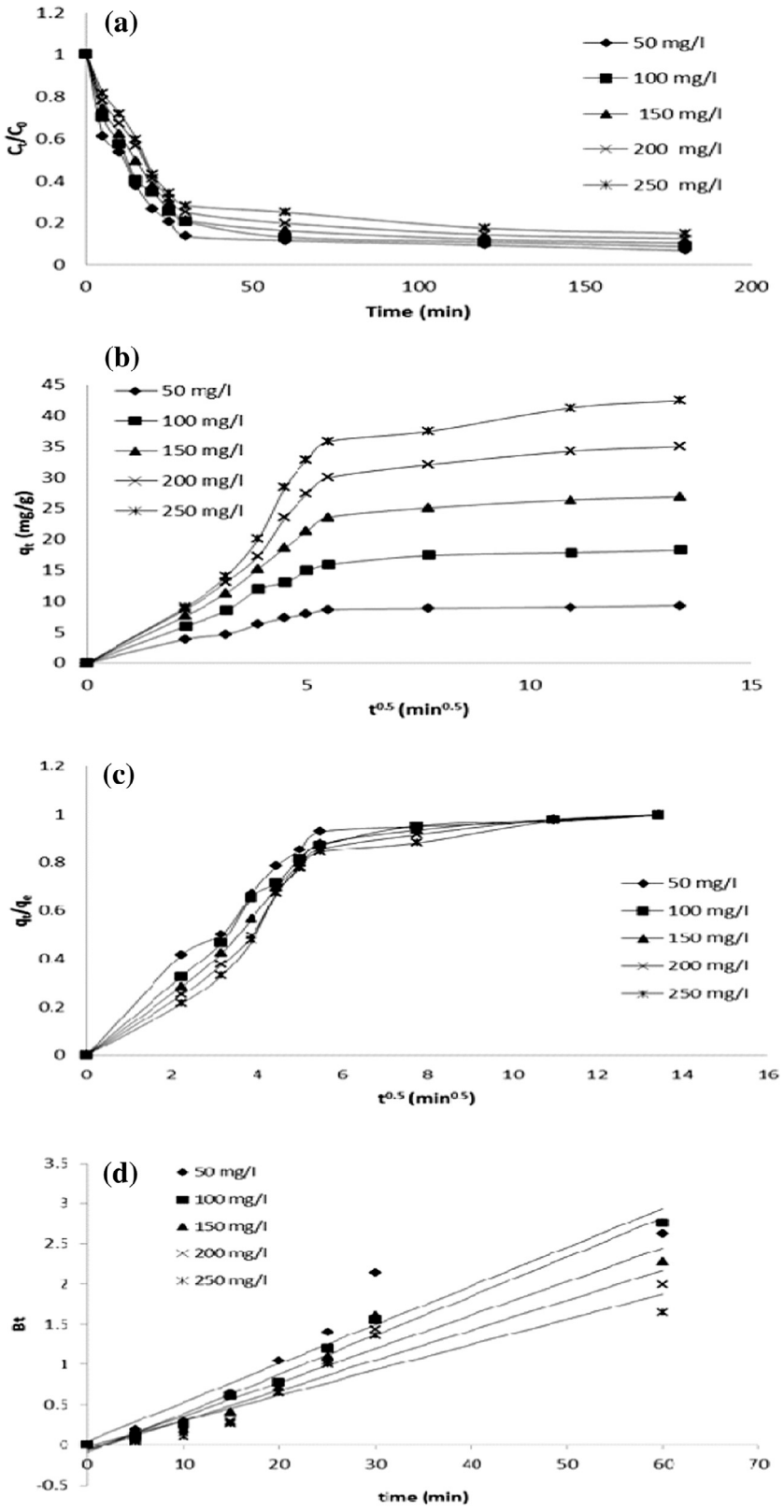

Figure 3 (a) Furusawa and Smith Plot; (b) Weber and Morris Plot; (c) Reichenberg and Helfferich plot and (d) Boyd plot.

The calculated *Bt* values were plotted against time and presented in Fig. 3(d). As seen these plots were linear at all concentrations but does not pass through the origin, conforming the film diffusion was the rate controlling one (Reichenberg, 1953). The pore diffusion coefficients D_p ($cm^2\ s^{-1}$) were obtained from the calculated Biot number values using Eq.

Table 7 Mass transfer parameters for adsorption of BM2 onto IGHSAC.

C_0 (mg l^{-1})	K_{id} (mg g^{-1} $min^{-0.5}$)	k_f	$D_f \times 10^{-8}$ (cm^2 s^{-1})	$D_p \times 10^{-6}$ (cm^2 s^{-1})	K_s (cm s^{-1})
50	0.0842	8.1695	4.9088	9.4448	0.0294
100	0.2741	14.755	4.5861	9.5233	0.0283
150	0.4122	21.606	4.2690	8.1881	0.0274
200	0.6427	26.776	4.0152	7.2848	0.0265
250	0.8874	30.926	4.0047	6.2049	0.0261

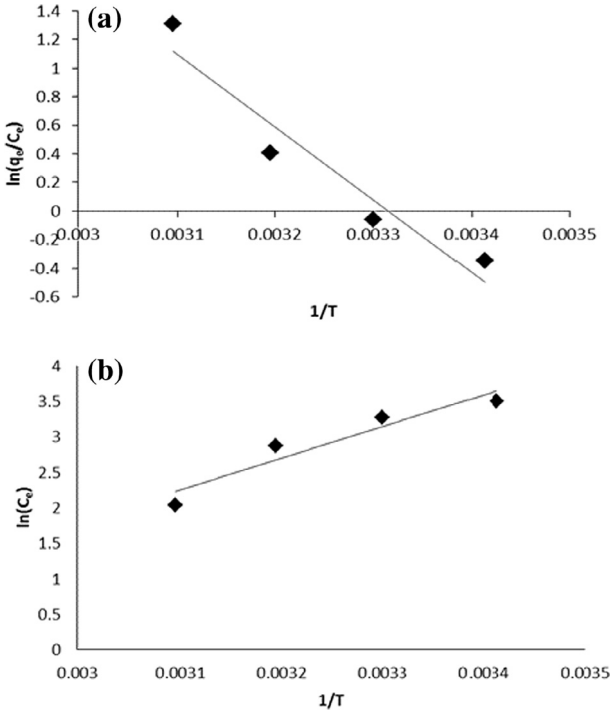

Figure 4 (a) Vant's Hoff plot and (b). Isoster plot.

(21) and presented in Table 7. Pore diffusion coefficient values are to be in the range of 10^{-11}–10^{-13} cm^2 s^{-1} for pore diffusion controlled adsorption mechanism (McKay and Poots, 1980) and the film diffusion coefficient values are to be in the range of 10^{-6}–10^{-8} cm^2 s^{-1} for film diffusion controlled adsorption mechanism (Michelson et al., 1975). Diffusion coefficients data (Table 7) revealed that the values of film coefficients are in the order of 10^{-8} and 10^{-6} cm^2 s^{-1}, respectively which indicated that the adsorption of BM2 onto IGHSAC was controlled purely by film diffusion at the studied concentration range which was supported by the results derived from Boyd plot.

3.5. Sorption thermodynamics

Thermodynamic parameters including the changes in Gibbs free energy ΔG^0 (J mol^{-1}) enthalpy ΔH^0 (J mol^{-1}) and entropy ΔS^0 (J mol^{-1} K^{-1}) can be calculated in order to illustrate the thermodynamic behaviour of adsorption process. The adsorption equilibrium constant (K_{ad}) can be correlated to the Gibbs free energy change ΔG^0 as (Smith and Van Ness, 1987):

$$\ln(K_{ad}) = \ln\left(\frac{q_e}{C_e}\right) = \frac{\Delta S^0}{2.303R} - \frac{\Delta H^0}{2.303R} \quad (31)$$

The change in entropy ΔS^0 (J mol^{-1} K^{-1}) and Gibbs free energy ΔG^0 (kJ mol^{-1}) can be related at constant temperature as follows:

$$\Delta G^0 = \Delta H^0 - T\Delta S^0 \quad (32)$$

where R is gas constant (8.314 J mol^{-1} K^{-1}) and T is the absolute temperature (K). The values of enthalpy and entropy changes were obtained from the slope and intercept of Fig. 4(a) and are given in Table 8. As observed that the adsorption of BM2 by IGHSAC was spontaneous and feasible with the negative values of ΔG^0. The positive standard enthalpy change ΔH^0 values confirmed the endothermic nature of the overall adsorption process. In general, the enthalpy change due to chemisorption (> 40 J mol^{-1}) is considerably larger than that of physi-sorption (< 40 J mol^{-1}). The higher order of magnitude of ΔH^0 (613.26 J mol^{-1}) conformed the chemisorption mechanism of BM2 molecules onto IGHSAC (Vinod and Aniruthan, 2001). The positive ΔS^0 values indicated that an increased disorder at the IGHSAC surface and dye solution interface with some structural changes in the IGHSAC particles as well as BM2 dye molecules during the adsorption process. This positive value also suggested the affinity BM2 molecules towards the IGHSAC particles and an increased degree of freedom of the adsorbed BM2 molecules (Senthilkumaar et al., 2006).

The apparent isosteric heat of adsorption ΔH_{is} (kJ kg^{-1}) can be calculated from the Clausius–Clapeyron equation:

$$\frac{d(\ln C_e)}{dT} = \frac{-\Delta H_{is}}{RT^2} \quad (33)$$

At constant q_e values the above equation becomes

$$-\Delta H_{is} = \frac{d(\ln C_e)}{d(1/T)} \quad (34)$$

ΔH_{is} was calculated from slope of the plot $\ln(C_e)$ versus $1/T$ (Fig. 4(b)). The positive values of ΔH_{is} confirmed the endothermic nature of the adsorption process (Lataye et al., 2009).

3.6. Process design

Single stage batch adsorber can be designed using empirical design procedures based on adsorption isotherms for predict-

Table 8 Thermodynamic parameters for adsorption of BM2 onto IGHSAC.

T (K)	ΔG (J mol^{-1})	ΔH (J mol^{-1})	ΔS (J mol^{-1} K^{-1})	ΔH_{is} (J kg^{-1})
293	−40560.05	613.26	140.52	4478.40
303	−41965.28			
313	−43370.52			
323	−44775.75			

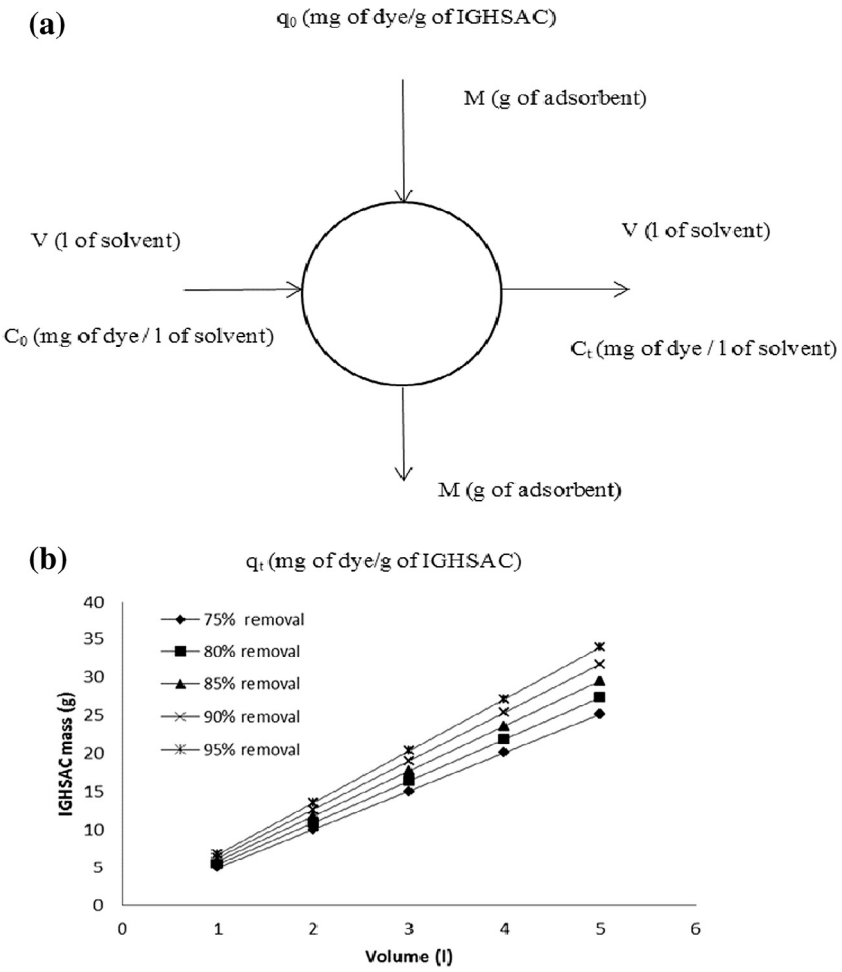

Figure 5 (a) Single stage batch adsorber and (b) adsorbent mass (g) against the volume of dye solution treated (l).

ing the adsorber size and performance (McKay et al., 1981; Vadivelan and Kumar, 2005). The schematic single stage batch adsorber is shown in Fig. 5(a). With the design objective as BM2 solution with initial concentration of C_0 (mg l^{-1}) and effective volume of V (l) to be reduced to C_t (mg l^{-1}) with the IGHSAC loading of M (g), mass balance equation can be written as follows

$$V(C_0 - C_t) = M(q_0 - q_t) \tag{35}$$

Since the equilibrium data for BM2 onto IGHSAC was explained well by Sips isotherm, q_t values at equilibrium (q_e) can be evaluated from Sips isotherm, therefore at equilibrium the Eq. (35) turned to

$$\frac{M}{V} = \frac{C_0 - C_e}{q_e} = \frac{C_0 - C_e}{\left(\frac{K_S q_{mS} C_e^{1/n_S}}{1 + K_S C_e^{1/n_S}}\right)} \tag{36}$$

Fig. 5(b) shows the plots obtained from Eq. (25) indicating the predicted amount of IGHSAC required for removing dye solution of initial concentration 150 mg l^{-1} to the extent of 75–90% colour removal at different solution volumes (1–5 l). For instance, the amount of IGHSAC required to reduce the colour of 150 mg l^{-1} to the degree of 90% was 6.3, 12.7, 19.1, and 25.4, 31.7 g for dye solution volumes of 1, 2, 3, 4 and 5 l respectively. Therefore Fig. 5(b) can be utilized to predict the amount of IGHSAC required for desired purification to the fixed concentration of 150 mg l^{-1}.

4. Conclusion

The adsorption of BM2 onto IGHSAC experimental data was analysed using different kinetic models by nonlinear regression. Error functions such as ERRSQ, HYBRID, MPSD, ARE and EABS were used to evaluate the SNE values and based on the minimum SNE values optimum parameter sets for kinetics were evaluated. The obtained parameter set was further analysed using R^2 and RMSE to gauge the goodness of fit. Avrami second-order model well described the kinetic data for different initial BM2 concentrations. Equilibrium concentrations were calculated with the equilibrium adsorption capacity obtained from the Avrami kinetic model. Different isotherms were investigated to understand the nature of adsorption with the help of nonlinear-SNE procedure. Adsorption equilibrium data was in good agreement with Sips and Hill isotherm models. The adsorption process was found to be controlled by film diffusion at the studied concentrations range. The thermodynamic study revealed that adsorption of

BM2 by IGHSAC was endothermic and spontaneous in nature. A single stage batch adsorber was designed using Sips isotherm constants to estimate the amount of IGHSAC required for desired purification.

References

Adamson, A.W., Gast, A.P., 1997. Physical Chemistry of Surfaces. Wiley-Interscience, New York.

Amran, M., Salleh, M., Mahmoud, D.K., Azlina, W., Karim, W.A., Idris, A., 2011. Cationic and anionic dye adsorption by agricultural solid wastes: a comprehensive review. Desalination 280, 1–13.

Baquero, M.C., Giraldo, L., Moreno, J.C., Suarez-Garcıa, F., Martınez-Alonso, A., Tascon, J.M.D., 2003. Activated carbons by pyrolysis of coffee bean husks in presence of phosphoric acid. J. Anal. Appl. Pyrol. 70, 779–784.

Bayramoglu, G., Yakup Arica, M., 2007. Biosorption of benzidine based textile dyes "Direct Blue 1 and Direct Red 128" using native and heat-treated biomass of Trametes versicolor. J. Hazard. Mater. 143, 135–143.

Blanchard, G., Maunaye, M., Martin, G., 1984. Removal of heavy metals from waters by means of natural zeolites. Water Res. 18, 1501–1507.

Cheung, C.W., Porter, J.F., McKay, G., 2000. Elovich equation and modified second-order equation for sorption of cadmium ions onto bone char. J. Chem. Technol. Biotechnol. 75, 963–970.

Daifullah, A.A.M., Girgis, B.S., Gad, H.M.H., 2004. A study of the factors affecting the removal of humic acid by activated carbon prepared from biomass material. Colloids Surf. A 235, 1–10.

Foo, K.Y., Hameed, B.H., 2010. Insights into the modeling of adsorption isotherm systems. Chem. Eng. J. 156, 2–10.

Forgacs, E., Cserhati, T., Oros, G., 2004. Removal of synthetic dyes from wastewaters: a review. Environ. Int. 30, 953–971.

Fu, Y., Viraragvahan, T., 2002. Dye biosorption sites in *Aspergillus niger*. Bioresour. Technol. 82, 139–145.

Girgis, B.S., Abdel-Nasser, A.E., 2002. Porosity development in activated carbons obtained from date pits under chemical activation with phosphoric acid. Microporous Mesoporous Mater. 52, 105–117.

Girgis, B.S., Yunis, S.S., Soliman, A.M., 2002. Characteristics of activated carbon from peanut hulls in relation to conditions of preparation. Mater. Lett. 57, 164–172.

Gupta, V.K., Mittal, A., Gajbe, V., Mittal, J., 2008. Adsorption of basic fuchsin using waste materials-bottom ash and deoiled soya-as adsorbents. J. Colloid Interface Sci. 319, 30–39.

Haghseresht, F., Lu, G., 1998. Adsorption characteristics of phenolic compounds onto coal-reject-derived adsorbents. Energy Fuels 12, 1100–1107.

Hanna, O.T., Sandall, O.C., 1995. Computational Methods in Chemical Engineering. Prentice-Hall International, New Jersey.

Hayashi, J., Kazehaya, A., Muroyama, K., Watkinson, A.P., 2000. Preparation of activated carbon from lignin by chemical activation. Carbon 38, 1873–1878.

Heiss, G.S., Gowan, B., Dabbs, E.R., 1992. Cloning of DNA from a Rhodococcus strain conferring the ability to decolorize sulfonated azo dyes. FEMS Microbiol. Lett. 99, 221–226.

Hill, A.V., 1910. The possible effects of the aggregation of the molecules of haemoglobin on its dissociation curves. J. Physiol. 40, 4–7.

Ho, Y.S., 1995. Adsorption of Heavy Metals from Waste Streams by Peat (Ph.D), University of Birmingham.

Ho, Y.S., 2004a. Pseudo-isotherms using a second order kinetic expression constant. Adsorpt. J. Int. Adsorpt. Soc. 10, 151–158.

Ho, Y.S., 2004b. Selection of optimum sorption isotherm. Carbon 42, 2115–2116.

Ho, Y.S., 2006a. Review of second-order models for adsorption systems. J. Hazard. Mater. B 136, 681–689.

Ho, Y.S., 2006b. Second-order kinetic model for the sorption of cadmium onto tree fern: a comparison of linear and non-linear methods. Water Res. 40, 119–125.

Ho, Y.S., McKay, G., 2003. Sorption of dyes and copper ions onto biosorbents. Process Biochem. 38, 1047–1061.

Ho, Y.S., Wang, C.C., 2004. Pseudo-isotherms for the sorption of cadmium ion onto tree fern. Process Biochem. 39, 759–763.

Ho, Y.S., Porter, J.F., McKay, G., 2002. Equilibrium isotherm studies for the sorption of divalent metal ions onto peat: copper, nickel and lead single component systems. Water Air Soil Pollut. 141, 1–33.

Hu, Z., Srinivasan, M.P., 1999. Preparation of high surface area activated carbons from coconut shell. Microporous Mesoporous Mater. 27, 11–18.

Huang, L., Kong, J., Wang, W., Zhang, C., Niu, S., Gao, B., 2012. Study on Fe(III) and Mn(II) modified activated carbons derived from Zizania latifolia to removal basic fuchsin. Desalination 286, 268–276.

Jagtoyen, M., Derbyshire, F., 1998. Activated carbons from yellow poplar and White oak by H_3PO_4 activation. Carbon 36, 1085–1097.

Jia-Guo, Xu, W.S., Chen, Y.L., Lua, A.C., 2005. Adsorption of NH3 onto activated carbon prepared from palm shells impregnated with H_2SO_4. J. Colloid Interface Sci. 281, 285–290.

Jin-Wha, K., Myoung-Hoi, S., Dong-Su, K., Seung-Man, S., Young-Shik, K., 2001. Production of granular activated carbon from waste walnut shell and its adsorption characteristics for Cu^{2+} ion. J. Hazard. Mater. B 85, 301–315.

Kasaoka, S., Sakata, Y., Tanaka, E., Naitoh, R., 1981. Design of molecular-sieve carbon. Studies on the adsorption of various dyes in the liquid phase. Int. Chem. Eng. 29, 734–742.

Kumar, K.V., Sivanesan, S., 2007. Sorption isotherm for safranin onto rice husk: comparison of linear and non-linear methods. Dyes Pigm. 72, 130–133.

Langmuir, I., 1918. The adsorption of gases on plane surfaces of glass, mica, and platinum. J. Am. Chem. Soc. 40, 1361–1403.

Lataye, D.H., Indra mani, Mishra Indra, Deo Mall, 2009. Adsorption of α-picoline onto rice husk ash and granular activated carbon from aqueous solution: equilibrium and thermodynamic study. Chem. Eng. J. 147, 139–149.

Lopes, E.C.N., dos Anjos, F.S.C., Vieira, E.F.S., Cestari, A.R., 2003. An alternative Avrami equation to evaluate kinetic parameters of the interaction of Hg(II) with thin chitosan membranes. J. Colloid Interface Sci. 263, 542–547.

Martin, M.J., Artola, A., Balaguer, M.D., Rigola, M., 2003. Activated carbons developed from surplus sewage sludge for the removal of dyes from dilute aqueous solutions. Chem. Eng. J. 94, 231–239.

McKay, G., Poots, V.J.P., 1980. Kinetics and diffusion processes in colour removal from effluent using wood as an adsorbent. J. Chem. Technol. Biotech. 30, 279–292.

McKay, G., Allen, S.J., McConvey, I.F., Otterburn, M.S., 1981. Transport processes in the sorption of colored ions by peat particles. J. Colloid Interface Sci. 80, 323–339.

Metcalf, Eddy, 2003. Wastewater Engineering, Treatment and Reuse. Tata McGraw-Hill, New Delhi.

Michelson, L.D., Gideon, P.G., Pace, E.G., Kutal, L.H., 1975. Removal of soluble mercury from wastewater by complexing techniques. US Dept. Ind. Water Res. Technol. Bull 74, 12–16.

Moreno-Castillaa, C., Carrasco-Marin, F.M.A., Lopez-Ramon, M.V., Alvarez-Merino, M.A., 2001. Chemical and physical activation of olive-mill wastewater to produce activated carbons. Carbon 39, 1415–1420.

Myers, R.H., 1990. Classical and modern regression with applications. PWSKENT 444–445, 297–298.

Namasivayam, C., Sangeetha, D., 2004. Equilibrium and kinetic studies of adsorption of phosphate onto $ZnCl_2$ activated coir pith carbon. J. Colloid Interface Sci. 280, 359–365.

Nawar, S.S., Doma, H.S., 1989. Removal of dyes from effluents using low-cost agricultural by-products. Sci. Total Environ. 79, 271–279.

Ncibi, M.C., 2008. Applicability of some statistical tools to predict optimum adsorption isotherm after linear and non-linear regression analysis. J. Hazard. Mater. 153, 207–212.

Ofomaja, A.E., 2011. Kinetics and pseudo-isotherm studies of 4-nitrophenol adsorption onto mansonia wood sawdust. Ind. Crops Prod. 33, 418–428.

Philip, C.A., 1996. Adsorption characteristics of micro porous carbons from apricot stones activated by phosphoric acid. J. Chem. Technol. Biotechnol. 67, 248–254.

Pollard, S.J.T., Fowler, G.D., Sollars, C.J., Perry, R., 1992. Low-cost adsorbents for waste and wastewater treatment: a review. Sci. Total Environ. 116, 31–52.

Radha, K.V., Regupathi, A., Arunagiri, T., Murugesan, T., 2005. Decolorization studies of synthetic dyes using Phanerochaete chrysosporium and their kinetics. Process Biochem. 40, 3343–3377.

Rafatullah, M., Sulaiman, O., Hashim, R., Ahmad, A., 2010. Adsorption of methylene blue on low-cost adsorbents: a review. J. Hazard. Mater. 177, 70–80.

Rajgopal, S., Karthikeyan, T., Prakash Kumar, B.G., Lima Rose, Miranda, 2006. Utilization of fluidized bed reactor for the production of adsorbents in removal of malachite green. Chem. Eng. J. 116, 211–217.

Ratkowski, D.A., 1990. Handbook of Nonlinear Regression Models. Marcel Dekker, New York.

Reichenberg, D.J., 1953. Properties of ion exchange resins in relation to their structure. III. Kinetics of exchange. Am. Chem. Soc. 75, 589–597.

Roderiguez-Reininoso, F., Molino Sabio, M., 1992. Activated carbons from lignocellulosic materials by chemical and/or physical activations: an overview. Carbon 30, 1111–1118.

Senthilkumaar, S., Kalaamani, P., Subburaam, C.V., 2006. Liquid phase adsorption of crystal violet onto activated carbons derived from male flowers of coconut tree. J. Hazard. Mater. B 136, 800–808.

Shi, W., Xu, X., Sun, G., 1999. Chemically modified sunflower stalks as adsorbents for colour removal from textile wastewater. J. Appl. Polym. Sci. 71, 1841–1850.

Sips, R., 1948. Combined form of Langmuir and Freundlich equations. J. Chem. Phys. 16, 490–495.

Sivarajasekar, N., Baskar, R., 2013. Adsorption of basic red 9 onto activated carbon derived from immature cotton seeds: isotherm studies and error analysis, desalination and water treatment, accepted manuscript, http://dx.doi.org/10.1080/19443994.2013.834518.

Sivarajasekar, N., Baskar, R., 2014. Adsorption of basic red 9 on activated waste *Gossypium hirsutum* seeds: process modeling, analysis and optimization using statistical design. J. Ind. Eng. Chem. 20, 2699–2709.

Sivarajasekar, N., Srileka, S., Samson arun prasath, S., Rabinson, S., 2008. Kinetic modeling for biosorption of methylene blue onto H_3PO_4 activated *Acacia arabica*. Carbon Lett. 9, 181–187.

Sivarajasekar, N., Balakrishnan, V., Baskar, R., 2009. Biosorption of a basic dye onto spirogyra. Univ. J. Chem. Technol. Metal. 44, 157–164.

Smith, J.M., Van Ness, H.C., 1987. Introduction to Chemical Engineering Thermodynamics. McGraw-Hill, Singapore.

Sobkowsk, J., Czerwi, A., 1974. Kinetics of carbon dioxide adsorption on a platinum electrode. J. Electroanal. Chem. 55, 391–397.

Sparks, D.L., 1989. Kinetics of Soil Chemical Processes. Academic Press, New York.

Srinivasan, A., Viraraghavan, T., 2010. Decolourization of dye wastewaters by biosorbents: a review. J. Environ. Manage. 91, 1915–1929.

Temkin, M.J., Pyzhev, V., 1940. Kinetics of ammonia synthesis on promoted iron catalysts. Acta Physicochim. URSS 12, 217–222.

Tsai, W.T., Chang, C.Y., Lee, S.L., Wang, S.Y., 2001. Thermo gravimetric analysis of corncob impregnated with zinc chloride for preparation of activated carbon. J. Therm. Anal. Calorim. 63, 351–357.

Ungarish, M., Aharoni, C., 1981. Kinetics of chemisorption: deducing kinetic laws from experimental data. J. Chem. Soc., Faraday Trans. 77, 975–985.

Vadivelan, V., Kumar, K.V., 2005. Equilibrium, kinetics, mechanism, and process design for the sorption of methylene blue onto rice husk. J. Colloid Interface Sci. 286, 90–100.

Vinod, V.P., Aniruthan, T.S., 2001. Sorption of tannic acid on zirconium pillared clay. J. Chem. Technol. Biotechnol. 77, 92–101.

Weber, T.W., Chakravorti, R.K., 1974. Pore and solid diffusion model for fixed bed absorbers. AIChE J. 20, 2228.

Weber Jr., W.J., Morris, J.C., 1963. Kinetics of adsorption on carbon from solution. J. Sanitary Eng. Div. Am. Soc. Civ. Eng. 89, 31–60.

Yeddou, R., Nadjemi, B., Halet, F., Ould-Dris, A., Capart, R., 2010. Removal of cyanide in aqueous solution by oxidation with hydrogen peroxide in presence of activated carbon prepared from olive stones. Miner. Eng. 23, 32–39.

Zhou, Y., Zhang, Q., Jin, Q., Ma, T., Hu, X., 2012. Heavy metal ions and organic dyes removal from water by cellulose modified with maleic anhydride. J. Mater. Sci. 47, 5019–5029.